

# Nanoscale

Accepted Manuscript



This is an *Accepted Manuscript*, which has been through the Royal Society of Chemistry peer review process and has been accepted for publication.

*Accepted Manuscripts* are published online shortly after acceptance, before technical editing, formatting and proof reading. Using this free service, authors can make their results available to the community, in citable form, before we publish the edited article. We will replace this *Accepted Manuscript* with the edited and formatted *Advance Article* as soon as it is available.

You can find more information about *Accepted Manuscripts* in the [Information for Authors](#).

Please note that technical editing may introduce minor changes to the text and/or graphics, which may alter content. The journal's standard [Terms & Conditions](#) and the [Ethical guidelines](#) still apply. In no event shall the Royal Society of Chemistry be held responsible for any errors or omissions in this *Accepted Manuscript* or any consequences arising from the use of any information it contains.

# Insulating to metallic transition of oxidized boron nitride nanosheet coating by tuning surface oxygen adsorption

Yufeng Guo\* and Wanlin Guo

*State Key Laboratory of Mechanics and Control of Mechanical Structures and MOE Key Laboratory for Intelligent Nano Materials and Devices, Institute of Nanoscience, Nanjing University of Aeronautics and Astronautics, Nanjing, 210016, China*

## Abstract:

Surface modification and functionalization are of fundamental importance in actual application of insulating coating, such as hexagon boron nitride (h-BN) nanosheet. Our first-principles calculations reveal that oxidized h-BN monolayer supported by Cu substrate exhibits metallic properties when O adatom vertically bonds with the B atom. This is mainly due to the hybridization of the  $p$  orbital of the BN layer and O adatom around the Fermi level. Charge transfer from the Cu substrate to the O atom stabilizes the formation of the vertical O-B bond. Injecting negative charges could trigger the migration of the O adatom from the B-N bond to B atom for metal or insulator-supported h-BN monolayer, which will lead to a metallic transition in the oxidized h-BN nanosheet. Our results provide a viable way to tune the electronic properties of surface h-BN coating through charge injection mediated O adsorption.

---

\*Corresponding author. Tel.: +86 25 84890513 Fax: +86 25 84895827. E-mail address: [yfguo@nuaa.edu.cn](mailto:yfguo@nuaa.edu.cn).

## 1. Introduction

Two-dimensional (2D) nanomaterials have attracted numerous scientific interests and attentions since the discovery of graphene materials and its extraordinary physical properties<sup>1</sup>. As one of the 2D-nanomaterials, a single hexagon boron nitride (h-BN) layer consists of a honeycomb basal plane with structural similarity to graphene, and possesses excellent thermal conducting<sup>2-4</sup>, mechanical properties<sup>5-7</sup> and high chemical stability<sup>8,9</sup>. Previous experimental and theoretical studies have shown that h-BN nanosheets hold promises for potential applications in electronic devices<sup>10,11</sup>, dielectric layer<sup>12-14</sup>, composite fillers<sup>15</sup> and surface coating<sup>16,17</sup>. Due to large band gap, h-BN nanosheets are good insulators<sup>18</sup>. Modulating the electronic properties of h-BN nanosheets is crucial for its application in electronic devices. Cutting BN nanosheets into nanoribbons, the band gaps of BN nanoribbons can be effectively tuned by applying external electric field<sup>19</sup>. Doping carbon atoms into BN nanosheets to form in-plane BCN hybrid nanostructures is another viable way for band gap and conductivity modulation<sup>20-23</sup>. Moreover, adsorption of hydrogen, fluorine atoms and functional moieties on the plane of BN nanostructures could also introduce significant modifications in electronic and magnetic properties<sup>24-27</sup>.

Hexagon BN nanosheets have excellent capability for oxidation resistance and could be used as surface protecting layer<sup>28</sup>. Although desorption of oxygen molecule is more favorable on a free-standing h-BN monolayer, oxygen atom prefers to adsorb and bind over a B-N bond of the h-BN monolayer, which leads to a remarkable decrease in the band gap<sup>29</sup>. When incorporated into an electronic or functional device,

the h-BN nanosheets are usually put or transferred on a variety of substrates. The physical or chemical coupling between BN nanosheet and substrate is actually inevitable. Recently a lot of studies have been conducted for ultrathin insulating layers supported by metal substrates because they are able to host electronic states decoupled from the metallic surface<sup>30-33</sup>. On the other hand, the B–N bonds, covalent in nature but with ionic characteristics, is sensitive to external charge and electric field. However, adsorption of oxygen atom on substrate-supported h-BN nanosheet and the effects of external charges remain unexplored. Further investigation on the electronic properties of substrate-supported h-BN nanosheet with oxygen adsorption is necessary for the development of h-BN nanosheet based surface functional coating.

In this study, we reveal two stable adsorption sites of O atom on Cu-supported h-BN monolayer by first-principles calculations. One site is on the B–N bond, another is vertically on the B atom that has lower binding energy than that on the B–N bond. The oxidized h-BN monolayer exhibits metallic properties when the O adatom vertically bonds with the B atom. Charge transfer from the underlying Cu substrate plays a key role in stabilizing O adsorption on the B atom. The metallic properties are enhanced by more O atoms adsorbing on the B atoms of the h-BN nanosheet. For Cu-supported h-BN bilayer and free-standing h-BN monolayer, there is only one favorable surface adsorption site where O atom is on the B–N bond. Injecting negative charges into Cu-supported h-BN monolayer, bilayer and free-standing h-BN monolayer could eliminate the energy barrier and prompts the O adatom migrating from the B–N bond to the B atom, and this will lead to a metallic transition in those

oxidized h-BN nanosheets.

## 2. Model and Method

We choose a rhombus unit cell with lattice length of 1.0224 nm where a  $4 \times 4$  h-BN monolayer (32 atoms) and a Bernal (AB) stacking h-BN bilayer (64 atoms) are placed on a  $4 \times 4$  Cu (111) substrate, respectively. The Cu (111) substrate (80 atoms) is composed of five layers and atoms in the bottom layer are fixed during structural relaxation, and there is a vacuum region larger than 2.2 nm in the direction perpendicular to the BN and substrate planes. According to experiment results, the lattice parameter for the h-BN is 0.2524 nm<sup>34</sup>. To match with the Cu substrate, the lattice of the h-BN nanosheets is stretched 1.3%. For Cu-supported h-BN bilayer, it can be considered as an h-BN monolayer placed on an insulating surface as the bottom BN sheet remains insulating on the Cu substrate<sup>31</sup>, so the combination of Cu and bottom BN monolayer (Cu/BN) could simulate an insulator substrate. All computations are performed within the framework of density-functional theory (DFT) as implemented in the VASP code by using the projector augmented wave method with the Perdew-Burke-Ernzerhof exchange-correlation functional<sup>35-37</sup>. The influence of van-der-Waals interactions is considered by using the Perdew-Burke-Ernzerhof exchange-correlation functional and the DFT-D2 method of Grimme<sup>36</sup> that consists in adding a semi-empirical dispersion potential to the conventional Kohn-Sham DFT energy. The whole system is relaxed by using a conjugate-gradient algorithm until the force on each atom is less than 0.1 eV/nm. Then an energy cutoff of 500 eV and special  $k$  points sampled on a  $6 \times 6 \times 1$  Monkhorst-Pack mesh<sup>39</sup> are employed to

calculate the exact energy. Our calculations show that the 1.3% stretching strain slightly influences the band structure and energy gap of the BN layers. Here the charge injection is realized by adding or subtracting a predetermined number of electrons to the total electrons of the system, which adjusts the charge neutrality level with a homogeneous background charge<sup>40</sup>.

### 3. Results and Discussion

First an O atom is placed on different surface locations of the Cu-supported h-BN monolayer, and then those systems are relaxed into equilibrium states. Finally, two stable O adsorption sites are obtained: one is vertically on the B atom and another is on the B-N bond, as shown by Fig. 1 (a) and (b). On the B atom, the O atom covalently bonds with the B atom and the length of the O-B bond is 0.138 nm, and the bonding B atom is lifted up from the BN plane. The average length of three neighbored B-N bonds is 0.16 nm, stretched about 8.3% comparing with other B-N bonds. For O adsorbing on the B-N bond, a BNO triangle ring is formed and the underlying B-N bond is stretched to 0.159 nm. The lengths of O-B and O-N bonds are 0.148 nm and 0.155 nm, respectively. The binding energy of O atom on the surface is calculated by  $E_b = E_{tot} - E_{bn/sub} - E_o$ , here  $E_{tot}$  is the total energy,  $E_{bn/sub}$  is the energy of the Cu-supported h-BN sheet, and  $E_o$  is the energy of a single O atom. The O binding energies on the B atom and B-N bond are -5.29 eV and -3.29 eV, respectively. The lower binding energy on the B atom represents stronger interaction and adsorption of O atom with the BN sheet. For Cu/BN-supported h-BN monolayer, there is only one stable surface adsorption site where O atom adsorbs on the B-N bond

and a BNO triangle ring forms, as shown in Fig. 1 (c). This favorable adsorption site of O atom is the same as that of free-standing h-BN monolayer<sup>29</sup>. The binding energy of O adatom on the B-N bond of the BN bilayer is -3.28 eV. The difference in the favorable adsorption sites between Cu-supported and Cu/BN-supported BN monolayers indicates an important role from the substrate.

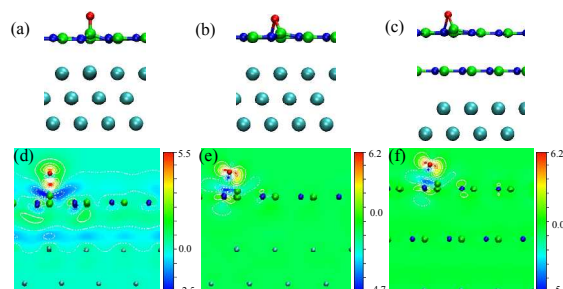


**Fig. 1** Stable optimized structures of O adsorbing on Cu-supported and Cu/BN-supported BN monolayers: (a) O atom on the B atom, (b) O atom on the B-N bond, and (c) O atom on the B-N bond of the Cu/BN-supported BN monolayer. The corresponding contour plots of 2D projection of charge density change  $\Delta\rho$  [in units of  $e/(\text{\AA})^3$ ] for O atom on (d) the B atom, (e) the B-N bond, and (f) the B-N bond of the Cu/BN-supported BN monolayer. The largest positive and negative values of the contour plots are shown in each panel. The red, green, blue and cyan dots are oxygen, boron, nitrogen and copper atoms, respectively.

To unveil the mechanism why O on the B atom is more stable than on the B-N bond, we calculate the charge density difference  $\Delta\rho = \rho_{tot} - \rho_{bn/sub} - \rho_o$ , here  $\rho_{tot}$  is the total charge density,  $\rho_{bn/sub}$  is the charge density of the Cu-supported h-BN sheet, and  $\rho_o$  is the charge density of a single O atom. Negative  $\Delta\rho$  denotes charge depletion and positive for charge accumulation. The contour plots of 2D projection of

charge density change  $\Delta\rho$  for O atom on the B atom and B-N bond of the BN monolayer are shown in Fig. 1 (d) and (e), respectively. For O on the B atom, there are a lot of charges accumulating at the O-B bond, and some charges transfer from the Cu surface to the O atom [Fig. 1 (d)]. On the contrary, no obvious charge exchange between O and Cu substrate is observed when O atom adsorbs on the B-N bond. The charge transfer from the Cu substrate to the O atom leads to a stronger O-B bond and lower binding energy. For the Cu/BN-supported BN monolayer, charge accumulation and depletion only distribute at the O adsorption site and the top BN layer, as shown in Fig. 1 (f). The bottom BN layer covered on the Cu substrate is actually an insulating surface, and no charge moves to the top layer. Therefore, the capability of substrate providing additional charges for the BN nanosheet determines the stability of O atom adsorbing on the B atom.

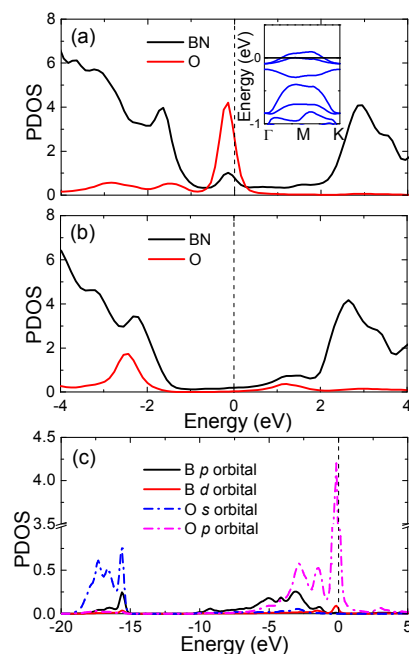


**Fig. 2** The projected DOS (in units of states/atom) of the  $p$  orbital of the Cu-supported BN monolayer and O atom for the O adatom on (a) the B atom

and (b) the B-N bond. (c) The projected PDOSs of the vertical O-B bond for the  $p$ ,  $d$  orbital of the B atom and  $s$ ,  $p$  orbital of the O atom. The inset shows the band structure of the BN monolayer where the O adatom is on the B atom and the Cu substrate is removed. The Fermi level is set to be zero.

The O adatom also gives rise to a significant change in electronic properties of the oxidized h-BN nanosheet. Fig. 2 (a) and (b) show the projected density of state (PDOS) of the  $p$  orbital of the Cu-supported h-BN monolayer and O atom with O adsorbing on the B atom and the B-N bond, respectively. There are peaks crossing the Fermi level for both BN layer and O atom when the O adatom is on the B atom. This kind of oxidized BN nanosheet exhibits metallic electronic properties. The peak of the PDOS around the Fermi level of the BN layer overlaps with that of the O adatom, which means the hybridization of the  $p$  orbital between them. When the substrate is removed, the left BN nanosheet with the O-B bond remains metallic, as shown by the inset in Fig. 2 (a). The formation of vertical O-B bond remarkably modifies the electronic properties of the oxidized BN nanosheet. Fig. 2 (c) shows the PDOSs of the vertical O-B bond including the  $p$ ,  $d$  orbital for the B atom and  $s$ ,  $p$  orbital for the O atom. The hybridization between the  $s$ ,  $p$  orbital of the O adatom and the  $p$  orbital of the bonded B atom is observed. A small PDOS peak of the  $d$  orbital of the B atom appears near the Fermi level, which overlaps with that of the  $p$  orbital of the O atom. This is the results of charge transfer from the Cu substrate. It should be mentioned that this vertical O adsorption site is unstable without the underlying substrate. Meanwhile, the Cu or Cu/BN-supported h-BN monolayer remains insulating when the

O adatom is on the B-N bonds or without O adsorption, as shown by Fig. 2 (b). To better understand the effects of O adsorption, the corresponding energy band structure of the Cu-supported h-BN monolayer with O adatom on the B atom are shown in Fig. 3. Here the bands crossing the contour plots are contributed by the B, N and O atoms, and band spectra weights and contributions from those atoms are highlighted by different colors. It is clearly shown that some bands around the Fermi level cross the contour plots. Accordingly, this oxidized BN monolayer after the B atom vertically bonds with the O atom becomes metallic, which is mainly attributed to the hybridization of the  $p$  orbitals of the BN layer and O adatom at the Fermi level. In other cases, the BN nanosheets are still insulating but the energy gap decreases when the O atom adsorbs on the B-N bond.

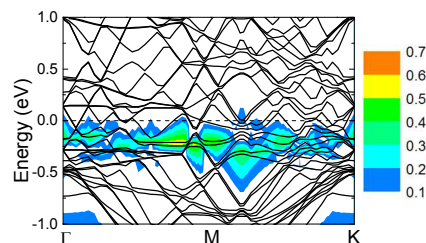


**Fig. 3 Band structure of the Cu-supported BN monolayer with O adatom on the B atom. The bands crossing the contour plots are contributed by the B, N and O atoms. The colors also indicate different spectra weights and contributions from the B, N and O atoms.**

In order to consider the influence from the variation in O adatom density, we have studied two O atoms adsorbing on the Cu-supported h-BN monolayer. Here two O atoms will become an O<sub>2</sub> molecule if they are too close or stay at near sites. The O<sub>2</sub>

molecule will move away from the BN plane and no bonding with B or N atom occurs. The O adatoms on the B atoms or the B-N bonds are stable when they are separated at a distance larger than the nearest sites of two B atoms or two B-N bonds. After structural relaxation, three typical stable adsorption states are achieved: two O atoms on two B atoms, one O atom on a B atom and another O atom on a B-N bond, and two O atoms on two B-N bonds. The two former states of the oxidized BN monolayer exhibit metallic electronic properties, as shown by the PDOSs in Fig. 4. For two O atoms on two B atoms, two peaks contributed by the BN monolayer and O atoms cross the Fermi level. The corresponding BN monolayer without the substrate is also metallic, as shown by the band structure of the inset. Similar trend is observed for the case that one O atom on the B atom and another O atom on the B-N bond, but with lower peak heights. The h-BN nanosheet is still insulating when two O atoms bind with two B-N bonds. Moreover, our calculations show that the total energy and binding energy of two O atoms on the B atoms are lower than that on the B-N bonds, suggesting the formation of vertical O-B bonds is still favorable with increasing the density of O adatoms.

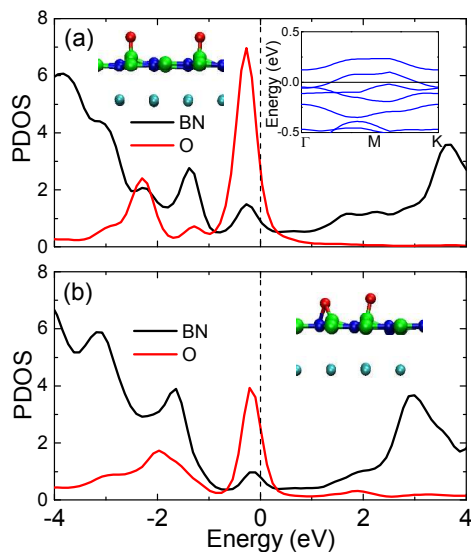


**Fig. 4** The projected DOS (in units of states/atom) of the  $p$  orbital of the Cu-supported BN monolayer and two O adatoms for (a) two O atoms on two B atoms, (b) one O atom on a B atom and another O atom on a B-N bond. The insets show the adsorption sites of the O atoms. The inset in (a) shows the band structure of the oxidized BN monolayer where two O atoms are on two B atoms and the Cu substrate is removed.

As the substrate-supported h-BN nanosheets exhibit different band structures upon the O adsorption, control of the adsorption site becomes a key issue to tune the electronic properties of the oxidized BN coating. In contrast to the Cu/BN-supported h-BN monolayer and suspended h-BN monolayer, there are two stable adsorption sites on the Cu-supported h-BN monolayer. The two stable adsorption sites are relaxed again for injecting negative and positive charges into the substrate. It is found that the O atom initially binding with the B-N bond moves to the B atom after structural relaxation under  $-1e$ . So we calculate the minimum energy paths (MEPs) for the O

atom moving from the B-N bond to the B atom by using the nudged elastic band method<sup>41</sup> based on the DFT technique. In the MEPs, the relative energy with respect to the total energy of an initial state is obtained. As shown in Fig. 5 (a), the energy barrier for the O migration from the B-N bond to B atom is 0.49 eV at the neutral state. Nevertheless, the energy barrier disappears through injecting one negative charge into the Cu substrate. Under -1e injection, the O atom on the B-N bond is unstable and binding on the B atom becomes the only favorable site. Injecting one positive charge leads to a converse situation. O adsorption on the B-N bond becomes more stable than that on the B atom. The energy barrier for O moving to the B atom is 0.35 eV while from the B atom to the B-N bond is 0.25 eV. Our further DFT calculations show that negative charge injection on the substrates could drive the O adatoms on the B-N bonds to move to the B atoms for both the Cu/BN-supported h-BN monolayer and suspended h-BN monolayer. Charge induced migration of O to B atom is also observed when more O atoms adsorb on the BN nanosheets. The change in the O adsorption demonstrates that charge injection could control the binding site of O atom on the substrate-supported h-BN nanosheets and the electronic properties of the h-BN coating are accordingly modified with the change of O adsorption site.

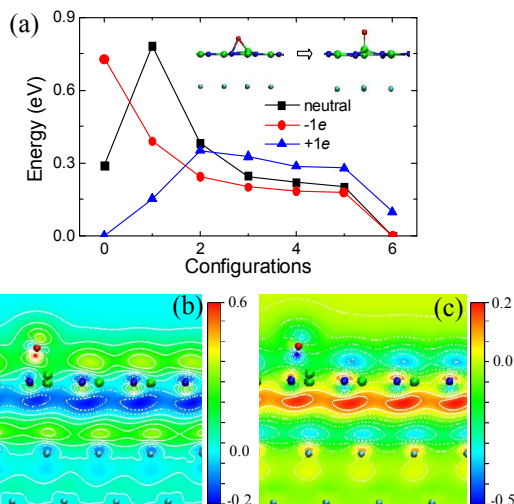


**Fig. 5 (a) Minimum energy pathways of the O atom on the B-N bond moving to the position on the B atom with and without charge injection on the Cu-supported BN monolayer. The insets show the initial and final configurations. Contour plots of 2D projection of charge density change  $\Delta\rho^{chg}$  [in units of  $e/(\text{\AA})^3$ ] for injecting (b)  $-1e$  and (c)  $+1e$  charge into the Cu-supported BN monolayer with O on the B-N bond. The denotation of contour plots and dots is the same as that in Figure 1.**

The underlying mechanism for adsorption modulation induced by external charge is elucidated in terms of the charge difference  $\Delta\rho^{chg}$  for O on the B-N bond, which is calculated by  $\Delta\rho^{chg} = \rho^{chg} - \rho^{unchg}$ , here  $\rho^{unchg}$  is the charge density of uncharged system, and  $\rho^{chg}$  is that of charged system. It can be seen from Fig. 5 (b) and (c) that under  $-1e$  injection charge depletion mostly distributes around the N atom bonding with the O adatom while charge accumulation mostly distributes at the O atom. Charge depletion at the N atom weakens the bonding state between N and O atom, and makes the O atom favorably bond with the B atom. For injecting  $+1e$ , charge

accumulation is dominating around the N atom, which strengthens the bonding state of N with O atom. The opposite response of O-N bond to negative and positive charge injection is consistent with the significant difference in the MEPs. For Cu/BN-supported BN monolayer under charge injection, the charge accumulation and depletion around the O adsorption site are similar to that of Cu-supported BN monolayer. This suggests that the charge induced adsorption site change of O atom is independent to the underlying substrate.

#### 4. Conclusion

Our extensive first-principles calculations present two stable O adsorption sites on Cu-supported h-BN monolayer. One is O atom on the B-N bond, and another site that has a lower binding energy between O and the underlying BN nanosheet is vertically on the B atom. Charge transfer from the metal substrate to the O atom is crucial for stabilization and formation of the vertical O-B bond. The adsorption of O atom on the B atom as well as the hybridization of the  $p$  orbital of the BN layer and O atom around the Fermi level leads to a metallic transition in the oxidized h-BN nanosheet. The migration of O atom from on the B-N bond to the B atom could be triggered by negative charge injection on metal or insulator-supported h-BN monolayer. These results provide insights into modulating the electronic properties of substrate-supported h-BN nanosheets through charge injection mediated O adsorption.

#### Acknowledgements

This work is supported by Program for New Century Excellent Talents in

University (NCET-13-0855), the 973 Program (2013CB932604, 2012CB933403), the NSF (11072109, 91023026), the Fundamental Research Funds for the Central Universities (No. NE2012005, NQ2013005) of China, and the Research Fund of State Key Laboratory of Mechanics and Control of Mechanical Structures (Nanjing University of Aeronautics and astronautics) (Grant No. 0413G01), and sponsored by Qing Lan Project.

## References

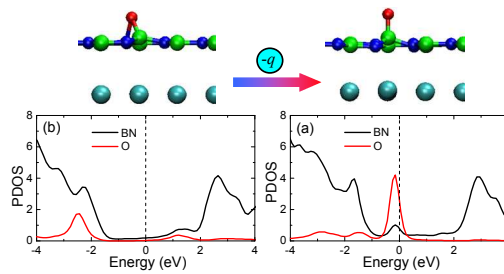
1. K. S. Novoselov, A. K. Geim, S. V. Morozov, D. Jiang, Y. Zhang, S. V. Dubonos, I. V. Grigorieva and A. A. Firsov, *Science*, 2004, **306**, 666.
2. C. Sevik, A. Kinaci, J. B. Haskins and T. Cagin, *Phys. Rev. B*, 2011, **84**, 085409.
3. J. W. Jiang and J. S. Wang, *Phys. Rev. B*, 2011, **84**, 085439.
4. J. W. Jiang, J. S. Wang and B. S. Wang, *Appl. Phys. Lett.*, 2011, **99**, 043109.
5. R. C. Andrew, R. E. Mapasha, A. M. Ukpong and N. Chetty, *Phys. Rev. B*, 2012, **84**, 125428.
6. L. Boldrin, F. Scarpa, R. Chowdhury and S. Adhikari, *Nanotechnology*, 2011, **22**, 505702.
7. H. Sxahin, S. Cahangirov, M. Topsakal, E. Bekaroglu, E. Akturk, R. T. Senger and S. Ciraci, *Phys. Rev. B*, 2009, **80**, 155453.
8. Y. Lin and J. W. Connell, *Nanoscale*, 2012, **4**, 6908.
9. K. A. Simonov, N. A. Vinogradov, M. L. Ng, A. S. Vinogradov, N. Martensson and A. B. Preobrajenski, *Surf. Sci.*, 2012, **606**, 564.

10. Y. Zhu, Y. Bando, L. Yin and D. Golberg, *Nano Lett.*, 2006, **6**, 2982.
11. C. R. Dean, A. F. Young, I. Meric, C. Lee, L. Wang, S. Sorgenfrei, K. Watanabe, T. Taniguchi, P. Kim, K. L. Shepard and J. Hone, *Nat. Nanotechnol.*, 2010, **5**, 722.
12. A. Mayorov, R. V. Gorbachev, S. V. Morozov, L. Britnell, R. Jalil, L. A. Ponomarenko, P. Blake, K. S. Novoselov, K. Watanabe, T. Taniguchi and A. K. Geim, *Nano Lett.*, 2011, **11**, 2396.
13. J. Xue, J. Sanchez-Yamagishi, D. Bulmash, P. Jacquod, A. Deshpande, K. Watanabe, T. Taniguchi, P. Jarillo-Herrero and B. J. LeRoy, *Nat. Mater.*, 2011, **10**, 282.
14. M. Yankowitz, J. Xue, D. Cormode, J. D. Sanchez-Yamagishi, K. Watanabe, T. Taniguchi, P. Jarillo-Herrero, P. Jacquod and B. J. LeRoy, *Nat. Phys.*, 2012, **8**, 382.
15. Y. Wang, Z. Shi and J. Yin, *J. Mater. Chem.*, 2011, **21**, 11371.
16. A. Pakdel, C. Zhi, Y. Bando, T. Nakayama and D. Golberg, *ACS Nano*, 2011, **5**, 6507.
17. J. Yu, L. Qin, Y. Hao, S. Kuang, X. Bai, Y.-M. Chong, W. Zhang and E. Wang, *ACS Nano*, 2010, **4**, 414.
18. D. Golberg, Y. Bando, Y. Huang, T. Terao, M. Mitome, C. Tang and C. Zhi, *ACS Nano*, 2010, **4**, 2979.
19. Z. H. Zhang and W. L. Guo, *Phys. Rev. B*, 2008, **77**, 075403.
20. L. Ci, L. Song, C. Jin, D. Jariwala, D. Wu, Y. Li, A. Srivastava, Z. F. Wang, K. Storr, L. Balicas, F. Liu and P. M. Ajayan, *Nat. Mater.*, 2010, **9**, 430.

21. T. W. Lin, C. Y. Su, X. Q. Zhang, W. Zhang, Y. H. Lee, C. W. Chu, H. Y. Lin, M.-T. Chang, F. R. Chen and L. J. Li, *Small*, 2012, **8**, 1384.
22. S. Dutta, A. K. Manna and S. K. Pati, *Phys. Rev. Lett.*, 2009, **102**, 096601.
23. S. Tang and Z. Cao, *Phys. Chem. Chem. Phys.*, 2010, **12**, 2313.
24. W. Chen, Y. Li, G. Yu, C. Z. Li, S. B. Zhang, Z. Zhou and Z. Chen, *J. Am. Chem. Soc.*, 2010, **132**, 1699.
25. Z. H. Zhang, X. C. Zeng and W. L. Guo, *J. Am. Chem. Soc.*, 2011, **133**, 14831.
26. A. Bhattacharya, S. Bhattacharya and G. P. Das, *Phys. Rev. B*, 2012, **85**, 035415.
27. A. Lopez-Bezanilla, J. Huang, H. Terrones and B. G. Sumpter, *Nano Lett.*, 2011, **11**, 3267.
28. Z. Liu, Y. Gong, W. Zhou, L. Ma, J. Yu, J. C. Idrobo, J. Jung, A. H. MacDonald, R. Vajtai, J. Lou and P. M. Ajayan, *Nat. Comm.*, 2013, **4**, 2541.
29. Y. Zhao, X. Wu, J. Yang and X. C. Zeng, *Phys. Chem. Chem. Phys.*, 2012, **14**, 5545.
30. F. Schulz, R. Drost, S. K. Hämäläinen and P. Liljeroth, *ACS Nano*, 2013, DOI: 10.1021/nm404840h.
31. S. Joshi, D. Eciija, R. Koitz, M. Iannuzzi, A. P. Seitsonen, J. Hutter, *et al.*, *Nano Lett.* 2012, **12**, 5821.
32. J. Repp, G. Meyer, F. E. Olsson and M. Persson, *Science* 2004, **305**, 493.
33. P. Liljeroth, J. Repp and G. Meyer, *Science* 2007, **317**, 1203.
34. C. S. Yoo, J. Akella, H. Cynn and M. Nicol, *Phys. Rev. B*, 1997, **56**, 140.
35. P. E. Blochl, *Phys. Rev. B* 1994, **50**, 17953.

36. G. Kresse and D. Joubert, *Phys. Rev. B* 1999, **59**, 1758.
37. J. P. Perdew, K. Burke and M. Ernzerhof, *Phys. Rev. Lett.* 1996, **77**, 3865.
38. S. Grimme, *J. Comput. Chem.*, 2006, **27**, 1787-1799.
39. H. J. Monkhorst and J. D. Pack, *Phys. Rev. B* 1976, **13**, 5188.
40. G. Makov and M. C. Payne, *Phys. Rev. B*, 1995, **51**, 4014.
41. G. Mills, H. Jonsson and G. K. Schenter, *Surf. Sci.* 1995, **324**, 305.

## Table of contents entry



Insulating to metallic transition of oxidized h-BN nanosheets supported by substrates

is induced by charge injection mediated O adsorption.